Proceedings of the 2005 IEEE
International Conference on Robotics and Automation
Barcelona, Spain, April 2005

Optimizing Leg Distribution Around the Body in Walking Robots*

Pablo Gonzalez de Santos, J. Estremera and E. Garcia.

Industrial Automation Institute-CSIC
Ctra. Campo Real Km 0,2
28500 Arganda del Rey, Madrid, Spain

pgds@iai.csic.es

***Abstract* - Walking-robot technology has reached an advanced stage of development, as has already been demonstrated by a number of real applications. However, further improvement is still needed if walking robots are to compete with traditional vehicles. Some potential improvements could be gained through optimization. Thus, this paper presents a method for distributing the legs around the robot's body such as to reduce the forces the legs must exert to support and propel the robot. The method finds through non-linear optimization techniques the middle leg displacement that nulls the difference between foot forces in a middle leg and a corner leg. A walking robot has been built to assess the theoretical results.**

Index Terms* - *Energy efficiency, legged locomotion, mobile robots, optimization methods.

I. INTRODUCTION

Walking robots have been investigated and developed intensively by many universities, research centers and companies since the late 70's. Most of them are laboratory prototypes, but there are also a few walking machines built for specific applications that have achieved acceptable reliability, such as the DANTE II [1], built for volcano inspection, the Aquarobot, designed for underwater surveying of seawalls [2], the ROWER, intended for naval construction [3], and the Timberjack, used for work in forests [4].

Generally speaking, however, walking robots have many shortcomings that bar them from wider use in industry and services. For instance, legged robots are still heavy, bulky, very slow and inefficient from the energy-expenditure point of view, which is a fundamental issue in autonomous robots. In other words, although legged robots have already demonstrated their capability to perform many tasks wheeled or tracked vehicles cannot handle, some features must still be improved before legged robots can meet present requirements in industry and services.

So far the designers of real walking robots have focused on the selection of the number of legs, the kinematic study of static stability and the design of leg mechanisms. There are, however, other issues related with walking-machine design that have received more timid scrutiny. For instance, it is easy to infer that legs in the mammal configuration can support heavy masses, while the insect configuration provides better static stability. Nonetheless, configuration notwithstanding, leg distribution around the body could help in improving some robot features. For instance, walking robots usually have parallelepiped bodies on which electronic equipment is loaded and legs are attached [1], [5], [6]; but body shape can determine static stability, as studied in [7]. Similarly, leg distribution around the body could also be adjusted to enable smaller actuators (smaller motors and/or smaller reducers) to be used to support the robot's weight, thereby reducing the weight, increasing the speed, or both at the same time.

All the legs on a walking robot are normally built on the same design, although mammals and insects possess very different rear and front (and sometimes middle) legs. The single standard leg design has many advantages in terms of design cost, replacements, modularity and so on. In quadrupeds leg distribution around the body is a simple thing, because not many combinations are available. Hexapods, on the other hand, offer a wider range of possibilities, as we will see below.

This article deals with the distribution of identical legs around a body. Such a leg distribution helps minimize the support forces exerted by the legs. Section II presents the foot forces exerted by a hexapod performing an alternating tripod gait. Next, Section III studies the influence of leg displacement in the force-distribution problem. Having determined the influence of leg displacement, Section IV presents a method for computing the leg displacements that minimize the maximum exerted foot force. Section V briefly presents the SILO6 walking robot, which was developed to perform humanitarian demining activities following a design drawn from the main result presented in this paper. Finally, some conclusions and future work are outlined.

II. FOOT FORCES ALONG A LOCOMOTION CYCLE

Walking robots are intrinsically slow machines, and machine speed is well known to depend theoretically on the number of legs the machine has [5]. Hence, a hexapod can achieve higher speed than a quadruped, and a hexapod achieves its highest speed when using a wave gait with a duty factor of $\beta = 1/2$, that is, using alternating tripods [8]. Although stability is not optimum when using alternating tripods, this gait is the most widely used by hexapods because of the speed they can achieve. These reasons made us focusing this work on alternating-tripod gaits. "Alternating tripods" means that two non-adjacent legs on one side and the middle leg on the opposite side alternate in supporting the robot.

To analyze the leg forces that a hexapod must exert, let us first consider an insect leg configuration as in Fig. 1a, where all leg workspaces lie in the same relative position with respect to the longitudinal axis of the body. In the robot situation shown in Fig. 1, the equilibrium equations that

* This work is supported by CICYT (Spanish Ministry of Education and Science) under Grants DPI2001-1595 and DPI2004-05824.

balance forces and moments –when three legs are in the support phase– are given by [9]:

$$\mathbf{AF=W} \tag{1}$$

where

$$\mathbf{A}=\begin{pmatrix} x_2 & x_3 & x_6 \\ y_2 & y_3 & y_6 \\ 1 & 1 & 1 \end{pmatrix} \tag{2}$$

$$\mathbf{F}=(F_2,\ F_3,\ F_6)^T \tag{3}$$

and

$$\mathbf{W}=(0,\ 0,\ -W)^{\mathbf{T}}. \tag{4}$$

F_i is the vertical ground-reaction force in foot i ($-F_i$ is the force foot i must exert against the ground), $(x_i,\ y_i)$ are the position components of foot i in the robot's reference frame (X, Y, Z) and W is the robot's weight.

For force-computation purposes, the robot is assumed to describe a continuous alternating-tripod gait that consists in two main phases. In the first phase, legs 1, 4 and 5 are in support and moving backwards at a constant speed (continuous gait), while legs 2, 3 and 6 are in their transfer phase moving forward to their next footholds (see Fig. 1a for leg definition). In the second phase, legs 1, 4 and 5 go to transfer while legs 2, 3 and 6 are in support. Notice that Fig. 1 illustrates this second phase. Each supporting leg follows a straight-line trajectory on the ground parallel to the trajectory of the other supporting legs. The distance through which the foot is translated relative to the body during the support phase is termed "leg stroke," R_x. This parameter defines the leg step of the gait. The stroke pitch, P_x, is the distance between the centers of the workspaces of the adjacent legs on one side. This is a fixed parameter that depends on the geometry of the walking robot and in this case coincides with the distance between adjacent-collateral leg reference frames (see Fig. 1). Some additional geometric parameters are the body length, L_B, the distance between the leg reference frames of non-collateral adjacent legs, D, and the distance from the foot trajectory to the origin of the leg reference frame, L. All these parameters and variables are defined in Fig. 1, and the relevant parameters for simulation purposes are given in Table I.

The alternating-tripod gait algorithm computes the foot components at any time given by:

$$\begin{pmatrix} x_i(k) & y_i(k) & z_i(k) \end{pmatrix}^T = G(k,i);\quad \text{for } i=1,..,6 \tag{5}$$

where k is the sample period, i is the leg number and G is the gait vector function defined by:

$$x_i(k)=\sigma(i)P_x+(-1)^{\xi\left(\frac{k}{N+1}\right)}R_x\cdot \left(\frac{1}{2}-\frac{1}{N-1}\left(((K-1)\bmod N)-1\right)\right); \tag{6}$$
$$\text{for } i=1,..,6; k=1,..,2N$$

$$y_i(k)=(-1)^{i+1}\left(\frac{D}{2}+L\right); \tag{7}$$
$$\text{for } i=1,..,6;\ k=1,..,2N$$

$$z_i(k)=\begin{cases} h\sin\left(\dfrac{\pi k}{N}\right)\left(1-\xi\left(\dfrac{k}{N+1}\right)\right)-H \\ \qquad \text{for } i=1,4,5;\ k=1,..,2N \\ -h\sin\left(\dfrac{\pi k}{N}\right)\xi\left(\dfrac{k}{N+1}\right)-H \\ \qquad \text{for } i=2,4,6;\ k=1,..,2N \end{cases} \tag{8}$$

where $2N$ is the number of samples in a locomotion cycle, H is the height of the body and h is the step height over the ground (see Fig. 1a and 1b). Function $\sigma(i)$ defines the displacement of the body attachment of leg i with respect to the center of the body reference frame (X, Y, Z) and is given by:

$$\sigma(i)=\begin{cases} 1;\ \text{for a front leg} \\ 0;\ \text{for a middle leg} \\ -1;\ \text{for a rear leg} \end{cases} \tag{9}$$

$\xi(x)$ is the function *fix*, which rounds the element x to the nearest integers towards zero, and *mod* represents the function module.

Equations (6) and (7) define analytically the $(x,\ y)$ trajectory of feet for an alternating-tripod gait. The component z_i must be over the ground for a leg in its transfer phase and on the ground for a leg in its support phase. The leg trajectory in this component can be defined in several

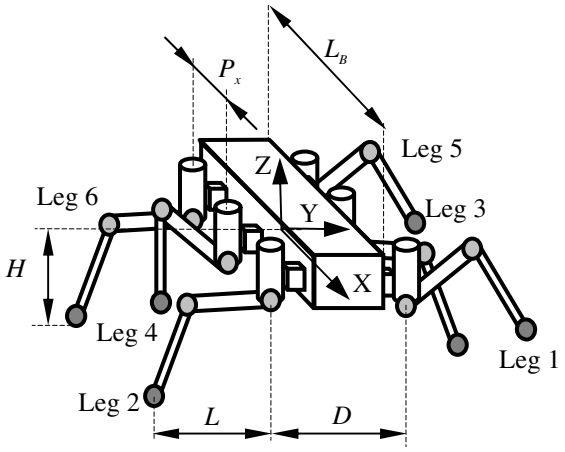

a)

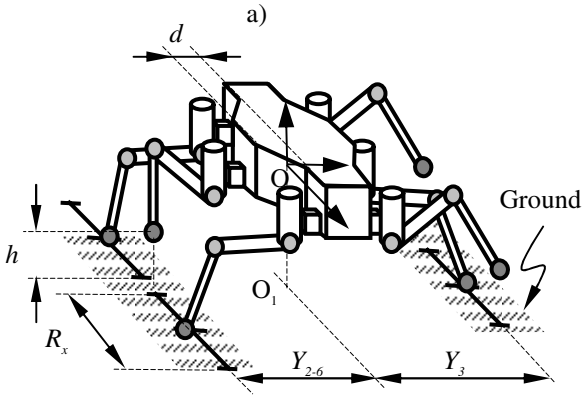

b)

Fig. 1 Geometric models of the walking robot.

very different ways: as a piecewise function, a polynomial function, a trigonometric function, and so on. For the sake of simplicity of formulation, the *sine* function has been chosen, and thus $z_i(k)$ is defined by (8).

With these foot positions, the foot forces along a whole locomotion cycle can be computed from (1) as:

$$\mathbf{F}=\mathbf{A}^{-1}\mathbf{W}\,. \tag{10}$$

For three legs in support, **A** is a square matrix, and therefore (10) gives a solution if and only if $det(A)\neq 0$. When the robot is supported by four to six legs, the pseudo-inverse matrix should be used [10].

The solution of (10) for the first half-locomotion cycle of the alternating-tripod gait is:

$$\begin{pmatrix} F_1(k) \\ F_4(k) \\ F_5(k) \end{pmatrix} = \begin{pmatrix} x_1(k) & x_4(k) & x_5(k) \\ y_1(k) & y_4(k) & y_5(k) \\ 1 & 1 & 1 \end{pmatrix}^{-1} \begin{pmatrix} 0 \\ 0 \\ -W \end{pmatrix} \tag{11}$$

for legs in their support phase (legs 1, 4 and 5 along the first half-cycle) and

$$\begin{pmatrix} F_2(k) \\ F_3(k) \\ F_6(k) \end{pmatrix} = \begin{pmatrix} 0 \\ 0 \\ 0 \end{pmatrix} \tag{12}$$

for legs in their transfer phase (legs 2, 3 and 4 along the first half-cycle). The solution for the second half-cycle can be computed similarly, and the closed solution along the whole locomotion cycle can be written as:

$$\begin{pmatrix} F_1(k) \\ F_4(k) \\ F_5(k) \end{pmatrix} = \left(1-\xi\left(\frac{k}{N+1}\right)\right) \begin{pmatrix} x_1(k) & x_4(k) & x_5(k) \\ y_1(k) & y_4(k) & y_5(k) \\ 1 & 1 & 1 \end{pmatrix}^{-1} \begin{pmatrix} 0 \\ 0 \\ -W \end{pmatrix}$$

$$\begin{pmatrix} F_2(k) \\ F_3(k) \\ F_6(k) \end{pmatrix} = \xi\left(\frac{k}{N+1}\right) \begin{pmatrix} x_2(k) & x_3(k) & x_6(k) \\ y_2(k) & y_3(k) & y_6(k) \\ 1 & 1 & 1 \end{pmatrix}^{-1} \begin{pmatrix} 0 \\ 0 \\ -W \end{pmatrix}$$

$$\text{for } k=1,..,2N \tag{13}$$

Equation (13) for the foot positions defined by (5) yields the foot reaction forces depicted in Fig. 2. In this example the locomotion cycle is 20 seconds and the sample period is 0.2 seconds.

This figure shows how the force distribution is symmetrical in the sense that left and right legs exert the same force considering the semi-cycle in which they are in support. Also, the front and rear legs complement each other in force, such that the sum of the forces of legs in the same tripod at any given time equal the weight of the robot, approximately 600 *N*. The maximum foot force for each leg is indicated in the upper right corner of the corresponding leg plot in Fig. 2. We can observe that the middle legs must exert a force of up to 294.3 **N**, while the corner legs only need to exert up to 227.78 **N**. If all the robot legs are based on the same design, this design should focus on the middle legs' requirements, and as a result the corner legs will be over-sized. However, the force a leg must exert or support depends heavily on that leg's foot position relative to the foot position of every other leg. Therefore, distributing legs around the body advantageously can help in properly distributing the foot forces among all the legs. The next section discusses this issue.

III. Leg Distribution Around the Robot's Body

When a legged robot is supported by a tripod as in Fig. 1, the middle leg in its support phase, for a given foot position, is carrying about half the robot's weight, while the two collateral legs in their support phase are carrying about one-fourth of the robot's weight. This can be observed in Fig. 2 for t = 5 seconds (legs 1, 4, and 5 in support phase) and t = 15 seconds (legs 2, 3 and 6 in support phase). These points correspond to the instants in which legs are in the middle of their workspaces. This circumstance is especially significant in traditional hexapod configurations, where all legs are placed at the same distance from the longitudinal axis of the robot's body.

Satisfactory force distribution and system homogenization can be achieved by shifting the middle legs' foot positions slightly from the body's longitudinal axis so that the middle legs support less weight and the corner legs increase their contribution to supporting the body.

The condition for sharing the weight of the robot evenly among the supporting legs for the case described above is given by (1) (see Fig. 1a):

$$\begin{pmatrix} P_X & -P_X & 0 \\ -Y_{2-6} & -Y_{2-6} & Y_3 \\ 1 & 1 & 1 \end{pmatrix} \begin{pmatrix} -W/3 \\ -W/3 \\ -W/3 \end{pmatrix} = \begin{pmatrix} 0 \\ 0 \\ -W \end{pmatrix} \tag{14}$$

That is, for every foot force assumed to be $-W/3$, feet 2 and 6 are at locations $(P_X, -Y_{2-6})$ and $(-P_X, -Y_{2-6})$, respectively, and foot 3 is at $(0, Y_3)$.

In (14) rows 1 and 3 are always satisfied and row 2 is satisfied if and only if:

$$Y_3 = 2\,Y_{2-6}\,. \tag{15}$$

That means the feet of the middle legs must be placed twice the distance from the longitudinal axis of the body as the feet of the corner legs. Possible leg configurations are shown in Fig. 3. Configuration a) resembles an insect configuration, and configuration b) resembles the crab configuration. Notice that by displacing the middle leg attachment points the support polygon increases; therefore, the static stability margins also increases.

Equation (15) gives the solution just for the specific robot pose in which footholds are symmetrical, as in the examples in Fig. 3; however, this study should be performed along a whole locomotion cycle, and the central leg-attachment point should be moved such that the maximum foot force in any middle leg equals the maximum foot force in any lateral leg. In this case, the legs can be designed to exert as little force against the ground as possible, thus helping to make the robot lighter or faster.

IV. Optimizing Leg Distribution Around the Robot's Body

One possible solution to decrease foot forces as pointed out in Section III consists in computing the middle-leg displacement that equals the maximum force exerted in every leg. For that, it is necessary to recalculate the foot forces for every foot position along a locomotion cycle. Then, the middle-leg displacement can be calculated that

will eliminate the difference between a middle leg's maximum force and a lateral leg's maximum force. The procedure is as follows:

The foot positions for generating an alternating-tripod gait are now given by:

$$\begin{pmatrix} x_i(k) & y_i^d(k) & z_i(k) \end{pmatrix}^T = G_d(k,i,d) \tag{16}$$

where k is the sample period, i is the leg number, d is the displacement of a middle leg with respect to a lateral leg along the direction of the Y-axis (see Fig. 1b) and G_d is the gait function given by:

$$x_i(k) = \sigma(i)P_x + (-1)^{\xi\left(\frac{k}{N+1}\right)} R_x \cdot \left(\frac{1}{2} - \frac{1}{N-1}\left(\left((K-1) \bmod N\right)-1\right)\right) \quad \text{for } i = 1,..6; k = 1,..,2N \tag{17}$$

$$y_i^d(k) = \begin{cases} (-1)^{i+1}\left(\frac{D}{2} + L\right); & for\ i = 1,2,5,6 \\ (-1)^{i+1}\left(\frac{D}{2} + L + d\right); & for\ i = 2,4 \end{cases} \tag{18}$$

$$z_i(k) = \begin{cases} h\sin\left(\frac{\pi k}{N}\right)\left(1 - \xi\left(\frac{k}{N+1}\right)\right) - H \\ \qquad \text{for } i = 1,4,5;\ k = 1,..,2N \\ -h\sin\left(\frac{\pi k}{N}\right)\xi\left(\frac{k}{N+1}\right) - H \\ \qquad \text{for } i = 2,4,6;\ k = 1,..,2N \end{cases} \tag{19}$$

where functions and parameters are those defined for (6)-(8). The component $y_i(k)$ and the gait function G are now written with the superscript d to indicate that they depend on the displacement of a middle leg. Note that the definitions of x_i and z_i coincide with the definitions of (6) and (8), respectively.

Now we can compute the foot forces given by (13) along a locomotion cycle as a function of parameter d (Notice that Fig. 2 was obtained for d = 0). Therefore, by varying the parameter d, we can match the maximum force exerted by each foot.

Figure 2 shows how the foot forces exhibit some symmetry, in that all four corner legs have the same maximum foot force and the two middle legs also get an equal maximum force. The problem is then reduced to finding the parameter d that yields:

$$\Phi(d) = 0 \tag{20}$$

where

$$\Phi(d) = \max_k(F_1(k,d)) - \max_k(F_3(k,d)). \tag{21}$$

In other words, we move the point where the middle legs

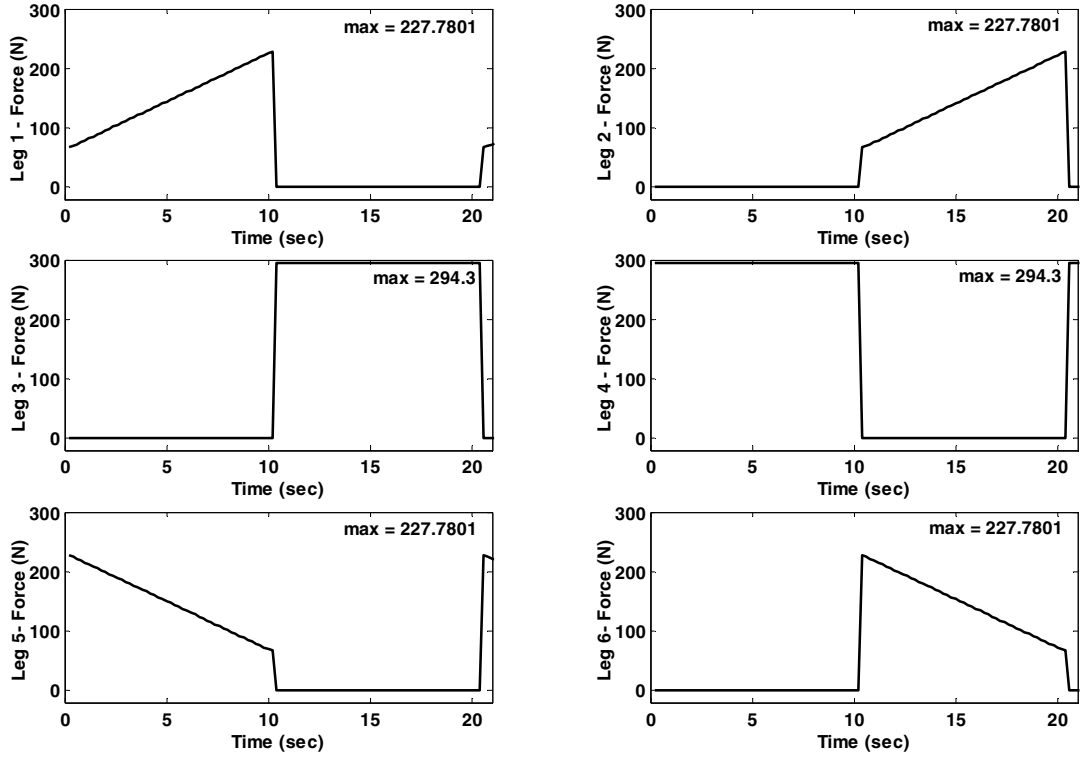

Fig. 2 Foot reaction forces for a locomotion cycle of the alternating-tripod gait.

(3 and 4) are attached until the maximum foot force in the middle legs equals the maximum foot force in the lateral legs (1, 2, 5 and 6).

The solution of a general non-linear equation as Φ is efficiently provided by the Gauss-Newton method [11]. This method requires an initial estimation of the solution and stops when it finds a local solution. For the geometric and mass parameters used in this study (see Table I), function Φ vanishes for d = 0.1561 m, which gives a maximum foot-force value of F_{max}= 249.95 N. Figure 4 plots the foot forces for the left legs. As mentioned above, the foot forces for the left and right legs are symmetrical. The right leg's foot forces have not been plotted for the sake of brevity.

Therefore, by moving the point where the middle leg is attached about d, we can reduce the maximum exerted foot forces by 44.35 N (from 294.3 N to 249.95 N) and thus reduce the maximum force by about 15.06%. This feature also influences actuator/gear-set selection and the robot's general features, especially speed and power consumption.

These findings are especially significant for robots based on orthogonal legs in which vertical foot force is applied directly by an independent actuator; when vertical support forces are minimized, smaller actuators can be used.

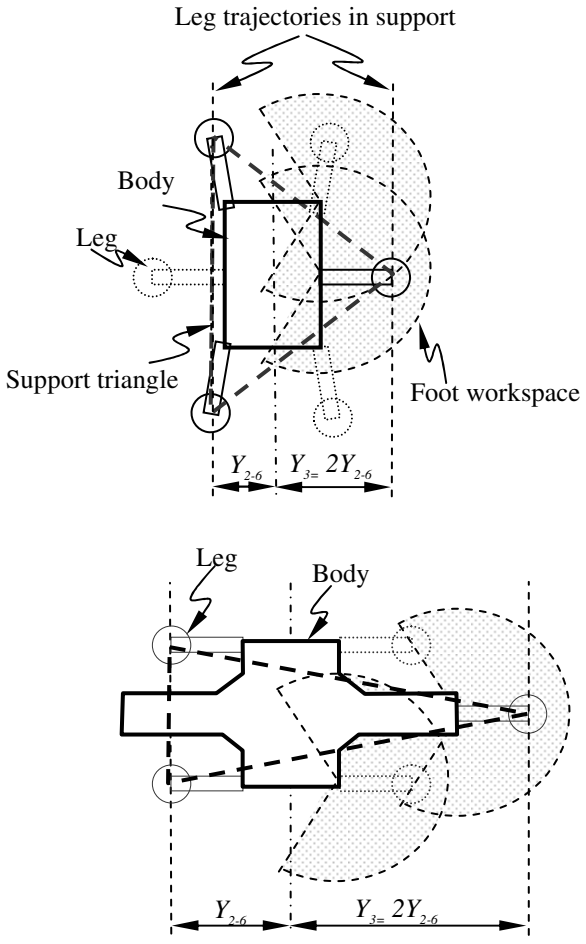

Fig. 3 Top view of two possible leg configurations: a) insect, b) crab.

V. Design of the SILO6 Walking Robot

The main findings herein have been used to design the SILO6 walking robot (see robot sketch in Fig. 1b and picture in Fig. 5). This is a six-legged robot developed as a mobile platform for the DYLEMA project [12]. The main aim of this project is to develop a locomotion system to integrate relevant technologies in the fields of legged robots and sensors to identify needs in humanitarian demining activities.

Energy autonomy is a mandatory feature in a trustworthy robot for humanitarian demining. A long-life power-supply unit (batteries or generator) is therefore required, but energy-efficient systems are still of paramount significance. Increasing the robot's energy efficiency is one of the main objectives in the design of the SILO6 walking robot.

The SILO6 has been configured as a hexapod, because hexapods can attain better speeds than quadrupeds. The middle legs have been separated from the longitudinal axis of the body by about 0.156 m, so that the maximum force exerted by any leg is minimized.

The legs have been based on a mechanism that can work as either an insect-type leg or a mammal-type leg. These two leg structures present complementary features. Mammal legs require less joint torques to support the body, but their static stability is very low. On the other hand, insect legs achieve better static stability, but at the cost of requiring high joint torques, which means higher energy expenditure. Selecting the adequate leg-type configuration is one more

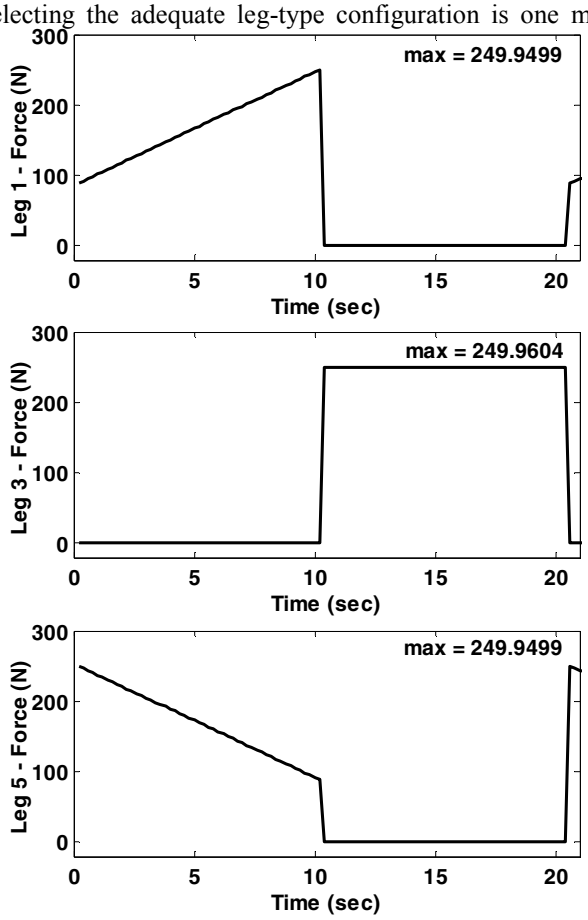

Fig. 4 Foot reaction forces in left legs for a locomotion cycle of an alternating-tripod gait when middle legs are shifted 0.1561 m.

way of improving robot efficiency, but it lies outside the scope of this paper.

Features of the SILO6 walking robot are summarized in Table I. Further details about the DYLEMA project and the SILO6 walking robot can be found in [12] and [13], respectively.

V. Conclusions

To date, walking robots have been developed just as showcases for the potential features of legged locomotion. It is high time to start optimizing robot design and control methods to make legged vehicles competitive with wheeled robots. This paper proposes a way of improving robot features through smaller actuators and lower energy expenditure. The method consists in reducing the maximum foot forces that a legged robot requires in order to support itself by placing the legs strategically around the robot's body. With lower maximum foot forces, designers can opt for smaller actuators or more lightweight robots, thus attaining higher speeds. The study shows that by displacing the middle legs on a hexapod, the maximum supporting foot forces can be reduced by 15.06%. All the traditional, well-known hexapod robots use parallelepiped bodies and thus cannot take advantage of the technique presented in this paper. The paper's authors were thus encouraged to build the SILO6 walking robot with the body shape shown in Fig. 5, which separates the middle legs from the lateral legs. Note that these results consider the robot's body leveled. With these premises, irregularities of the terrain including slopped terrain do not affect the computation of foot forces and thus results are independent of the terrain features.

A future step forward will be the computation of optimum leg poses for minimizing joint torques and thus further minimizing energy expenditure.

References

[1] J.E. Bares and D.S.Wettergreen, "Dante II: Technical description, results and lesson learned," *The International Journal of Robotics Research*, vol. 18, no. 7, pp. 621-649, 1999.

[2] J. Akizono, M. Iwasaki, T. Nemoto, and O. Asakura, ''Development on walking robot for underwater inspection,'', *Proceedings of the International Conference on Advanced Robotics*, Springer-Verlag, pp. 652–663, 1989.

[3] P. Gonzalez de Santos, M.A. Armada and M.A. Jimenez, "Ship building with ROWER," *IEEE Robotics and Automation Magazine*, vol. 7, no. 4, pp. 35-43, 2000.

[4] Plustech Inc. Available in http://www.plustech.fi/Walking1.html, 2004,

[5] K.J. Waldron, V.J. Vohnout, A. Perry and R.B. McGhee, "Configuration design of the adaptive suspension vehicle," *The International Journal of Robotic Research*, vol. 3, no. 2, pp. 37-48, 1984.

[6] K. Nonami, Q.J. Huang, D. Komizo, N. Shimoi, and H., Uchida, "Humanitarian mine detection six-legged walking robot," *Proceedings of the 3rd International Conference on Climbing and Walking Robots*, pp. 861-868, Madrid, Spain, 2000.

[7] A. Schneider, I. Zeidis and K. Zimmermann, "Comparison of body shapes of walking machines in regards to stability margins," *Proceedings of the 3rd International Conference on Climbing and Walking Robots*, pp. 275-281, Madrid, Spain, 2000.

[8] S.M. Song, and K.J. Waldron, "MACHINES THAT WALK: The Adaptive Suspension Vehicle," The MIT Press Series in AI, 1989.

[9] C.A. Klein, and S. Kittivatcharapong, "Optimal force distribution for the legs of a walking machine with friction cone constraints," *IEEE Transactions on Robotics and Automation*, vol. 6, no. 1, pp. 73-85, 1990.

[10] C.A. Klein and T.S. Chung, "Force interaction and allocation for the legs of a walking vehicle," *IEEE Journal of Robotics and Automation*, vol. RA-3, no. 6, pp. 546-555, 1987.

[11] MATLAB, The Language of Technical Computing, The Math Works Inc. 1996.

[12] P. Gonzalez de Santos, E. Garcia, J. Estremera and M.A. Armada, "DYLEMA: Using walking robots for landmine detection and location," *International Journal of System Science*, in press, 2004.

[13] P. Gonzalez de Santos, E. Garcia, J.A. Cobano and A. Ramirez, "SILO6: A Six-Legged Robot for Humanitarian De-Mining Tasks," 6th Biannual World Automation Congress (WAC 2004), pp. 515-521, Seville, Spain, June 28 - July 1, 2004.

TABLE I
SILO6 FEATURES.

Body	Dimensions (m)	Length (L_B)		0.88
		Width	Front/rear (D)	0.38
			Middle	0.635
		Height		0.26
		Stroke Pitch (P_x)		0.365
	Mass (kg)			≈20
	Speed (m/s)			0.05
Leg	Link	1	2	3
	Length (m)	0.094	0.250	0.250
	Stroke (R_x) (m)			0.2
	Mass (kg)			≈5
	Foot speed (m/s)	Transfer phase		0.140
		Support phase		0.05
Robot	Total mass including manipulator (M) (kg)			60

Fig. 5 The SILO6 walking robot